Available online at www.sciencedirect.com
SCIENCE DIRECT®
Virology 326 (2004) 90–102
VIROLOGY
www.elsevier.com/locate/yviro

Analysis of a viral replication repressor: sequence requirements for a large symmetrical internal loop

Jiuchun Zhang, Robert M. Stuntz, and Anne E. Simon*

Department of Cell Biology and Molecular Genetics, University of Maryland, College Park, MD 20742, USA

Received 16 March 2004; accepted 7 May 2004

Abstract

Nearly all members of the *Carmovirus* genus contain a structurally conserved 3′ proximal hairpin (H5) with a large internal symmetrical loop (LSL). H5 has been identified as a repressor of minus-strand synthesis in a satellite RNA (satC), which shares partial sequence similarity with its helper virus *Turnip crinkle virus* (TCV). Repression was due to sequestration of the 3′ end mediated by base pairing between 3′ end sequence and the 3′ side of the LSL (G. Zhang, J. Zhang and A. E. Simon, J. Virol., in press). Single site mutational analysis and in vivo genetic selection (SELEX) of the 14 base satC H5 LSL indicated specific sequences in the middle and upper regions on both sides of the LSL are necessary for robust satC accumulation in plants and protoplasts. Fitness of wild-type satC and satC LSL mutants to accumulate in plants, however, did not necessarily correlate with the ability of these RNAs to replicate in protoplasts. This suggests that the LSL might be involved in processes in addition to repression of minus-strand synthesis.
© 2004 Elsevier Inc. All rights reserved.

Keywords: RNA virus replication; Satellite RNA; Replication repressor; RNA structure; In vivo SELEX

Introduction

Positive-strand RNA viruses contain *cis*-acting elements in their 5′ and 3′ untranslated regions (UTRs) that play indispensable roles in replication of the viral genome (Buck, 1996; Duggal et al., 1994). Core promoters, which recruit viral encoded RNA-dependent RNA polymerases (RdRp) to transcription initiation sites, are often located at the 3′ ends of both strands (Buck, 1996; Chapman and Kao, 1999; Deiman et al., 1998; Duggal et al., 1994; Sivakumaran et al., 1999; Song and Simon, 1995). Elements that regulate promoter efficacy, including enhancers and repressors, can be located either proximal or distal to the core promoter (Barton et al., 2001; Herold and Andino, 2001; Khromykh et al., 2001; Klovins et al., 1998; Nagy et al., 1999, 2001; Panavas and Nagy, 2003; Pogany et al., 2003; Ray and White, 1999, 2003; You et al., 2001; Zhang et al., in press). Additional *cis*-acting elements have also been identified that function as RNA chaperones and assist in replicase maturation (Quadt et al., 1995; Vlot et al., 2001). Most of these *cis*-acting elements share little sequence similarity or structural features between unrelated viruses and, where examined, appear to function through direct interaction with other sequence elements or viral or cellular proteins (Dreher, 1999; Duggal et al., 1994; Fabian et al., 2003; Haldeman-Cahill et al., 1998; Klovins et al., 1998; Melchers et al., 1997; Pillai-Nair et al., 2003; Singh and Dreher, 1998; Sivakumaran et al., 1999; White et al., 1992; Williams et al., 1999; Yu et al., 1999; Zhang et al., in press).

Much attention has been focused on the 3′ UTR of plus-strand RNA viruses. 3′ UTR elements such as tRNA-like structures or other hairpins, poly(A) tails, or heteropolymeric single-stranded sequences have important roles in diverse viral functions including promotion of minus-strand synthesis, regulation of replicase access to the site of transcription initiation, telomeric-type protection of 3′ end sequences, packaging nucleation signals, modulation of translation, and targeting of RNA to specific subcellular sites (Buck, 1996; Dreher, 1999). Because many of these functions have related effects on genome amplification,

* Corresponding author. Department of Cell Biology and Molecular Genetics, University of Maryland, 1109 Microbiology Building, College Park, MD 20742. Fax: +1-301-314-7930.

E-mail address: Anne_Simon@umail.umd.edu (A.E. Simon).

0042-6822/$ - see front matter © 2004 Elsevier Inc. All rights reserved.
doi:10.1016/j.virol.2004.05.006

subviral RNA replicons have proven useful for identifying elements involved primarily in replication.

The association of *Turnip crinkle virus* (TCV) (family *Tombusviridae*, genus *Carmovirus*) with several subviral RNA replicons makes it an ideal system with which to identify sequences specifically involved in RNA replication. The 4054-base genomic RNA contains five open reading frames including p28 and its readthrough product, p88, which comprise the viral RdRp. p88 alone contains RNA polymerase activity that is specific for TCV-associated RNAs in an in vitro (cell-free) system (Rajendran et al., 2002). Two subgenomic (sg)RNAs are thought to be synthesized from minus strands of TCV genomic RNA: a 1.7-kb sgRNA that encodes two movement proteins, p8 and p9, and a 1.45-kb sgRNA that directs the synthesis of the single viral capsid protein (Hacker et al., 1992; Li et al., 1998).

In addition to its genomic RNA, TCV is associated with several dispensable noncoding subviral RNAs including satC (356 bases) and satD (194 bases). SatC is an unusual chimeric RNA sharing 88% similarity with nearly full-length satD at its 5′ end. The 3′ portion of satC originated from two regions in the 3′ end of TCV, with the related regions sharing 94% sequence similarity (Simon and Howell, 1986) (Fig. 1A).

The core promoter (Pr) for synthesis of satC minus strands has been identified as a 3′ terminal stem-loop flanked by the sequence (CCUGCCC-OH), which is also found at the 3′ end of TCV genomic RNA and satD (Carpenter and Simon, 1998; Carrington et al., 1989; Simon and Howell, 1986; Song and Simon, 1995; Stupina and Simon, 1997; Fig. 1B). Recently, a hairpin (H5) located proximal to the core hairpin promoter of satC has been identified as a repressor of minus-strand synthesis (Zhang et al., in press). H5 contains a large, 14-base symmetrical internal loop (LSL) that is responsible for its repressor activity. Repression was mediated by base pairing between four of the seven bases on the 3′ side of the LSL (5′GGGC) and the satC 3′ terminal bases (GCCC-OH) (Zhang et al., in press). Deletion of the satC 3′ terminal three cytidylates or mutations that altered the 3′ side of the LSL or H5 structure enhanced synthesis of both full-length and aberrantly initiated complementary strands in an in vitro transcription assay using purified TCV p88. Compensatory exchanges of putative base pairs between the 3′ side of the LSL and 3′ terminal bases restored near normal accumulation of complementary strands in this assay. In addition, solution structure analysis indicated that deletion of the 3′ terminal three bases (CCC-OH) had a substantial effect on the structure of H5 and 3′ proximal sequences without major modification of other sequences. These results suggested that H5 represses minus-strand synthesis by sequestering the satC 3′ terminus from the RdRp through the interaction between the 3′ terminus and the LSL. Structurally similar Pr and H5 elements are also located in identical positions in nearly all other carmoviruses (Zhang et al., in press).

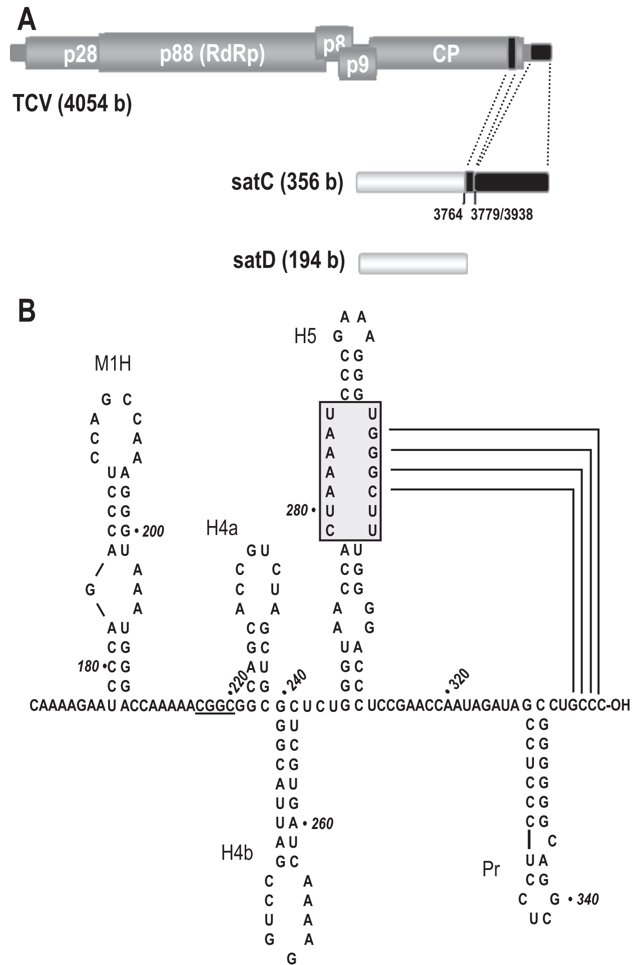

Fig. 1. Sequence and structure of the 3′ end of satC. (A) Schematic representations of TCV and two associated satellite RNA, satC and satD. Similar regions are shaded alike. The blackened portions in TCV comprise the 3′ 166 bases of satC (94% similarity) (Simon and Howell, 1986). (B) Structure of the 3′ region of satC (positions 170–356). Numbering of bases is from the 5′ end. The names of the hairpins are given. The large symmetrical loop (LSL) of H5 is boxed and shaded. Base pairing between the 3′ side of the LSL and the 3′ terminal bases of satC that results in repression of minus-strand synthesis in vitro is shown. Pr, core promoter required for satC minus-strand synthesis. H4a and H4b, hairpins of unknown function structurally and positionally conserved in TCV and several other carmoviruses. M1H, hairpin required on plus strands to juxtapose single-stranded sequences at its base, which interferes with TCV virion formation enhancing virus movement (Zhang and Simon, 2003a, 2003b). Underlined bases were identified as a derepressor, proposed to free the 3′ terminus from interaction with H5 by base pairing with the satC 3′ end (Zhang et al., in press).

For this study, we performed site-specific mutagenesis and in vivo genetic selection (in vivo SELEX) to analyze sequence requirements of the satC H5 LSL for satC accumulation in vivo. Our findings demonstrate that nearly all positions in the middle and upper regions of the LSL are crucial for replication of satC in protoplasts and fitness to accumulate in vivo. Our results also suggest that H5 might have additional functions besides that of repressor of minus-strand synthesis.

Results

Single base changes on both sides of the H5 LSL can substantially reduce accumulation of satC in protoplasts

Our recent study (Zhang et al., in press) indicated that alteration of three bases [U296C, G297A, and G299A; denoted as wild-type (wt) base, position, mutant base] on the 3′ side of the LSL in the same construct reduced satC accumulation to below detectable levels in protoplasts. Not addressed in this study was the importance of individual alterations at these positions and at other bases on both sides of the LSL. To determine experimentally the importance of specific positions in the LSL for satC accumulation in vivo, single base alterations at each position were generated in a full-length satC clone (Fig. 2A). Transcripts synthesized from the mutant constructs were inoculated onto *Arabidopsis thaliana* protoplasts along with TCV helper virus, and accumulation of satC after 40 h was determined by RNA gel blots.

SatC containing alterations at positions 279 and 285, the upper and lowest position in the LSL 5′ side, were viable, although different mutations at these positions had different effects on satC accumulation. SatC containing U285A and U285G accumulated to only 8% or 2% of wt satC, respectively, while U285C was better tolerated, only reducing satC levels to 59% of wt. These results suggest that closing the upper position of the LSL by alterations allowing base pairing (U285A and U285G) was strongly detrimental to H5 function. In contrast, alterations in the LSL 5′ side that permit base pairing in the lowest position of the LSL (C279G, C279A) accumulated to 40% and 134% of wt levels, respectively, indicating that closure of the lowest position of the LSL is permitted. Alteration of the four adenylates on the 5′ side of the LSL (positions 281–284)

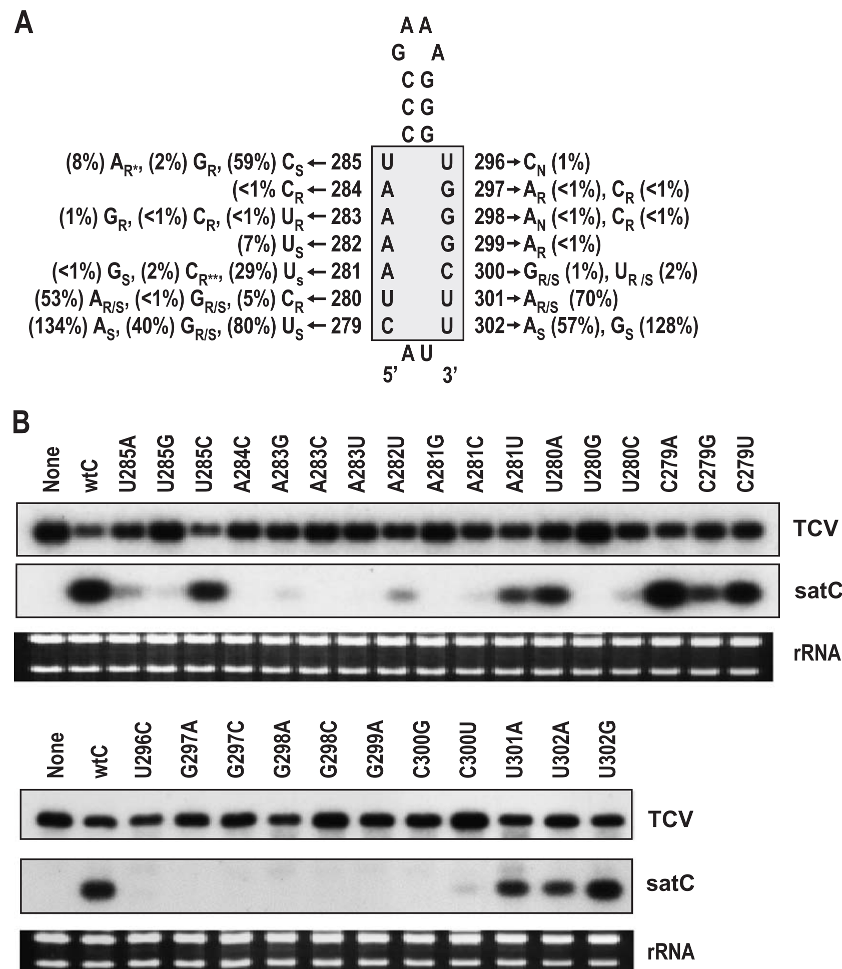

Fig. 2. Single site mutational analysis of the satC H5 LSL in vivo. (A) Location of the mutations constructed in satC and summary of the effects on satC accumulation in protoplasts and plants. Numbering of bases (from the 5′ end) is shown. Accumulation in protoplasts of the individual mutants expressed as a percentage of wt satC levels is given in parentheses. Stability of the mutations in plants was assayed at 21 dpi and is denoted by subscripts as follow: N, no satC species detected by PCR; R, mutations reverted to wt in all recovered clones; S, mutations were always maintained; R/S, mutations either reverted to wt or were maintained (see Table 1). R* associated with U285A denotes mutation either reverted to the wt U or a C. R** associated with A281C denotes mutation either reverted to the wt or a U. (B) Representative RNA gel blot of mutant satC and helper virus (TCV) plus strands. Total RNA was extracted at 40 hpi from *Arabidopsis* protoplasts. Gels were stained with ethidium bromide before blotting to reveal rRNA loading control (below the blot). None, no added satC. wtC, wt satC.

was generally detrimental with the exception of A281, the 5′ most adenylate, which retained 30% of wt accumulation when converted to a uridylate (A281U).

Mutations generated in the 3′ LSL GGGC (positions 297–300), which were previously determined to base pair with 3′ terminal bases in vitro (Zhang et al., in press), were highly detrimental as expected. In addition, U296C and U301A, which flank the LSL bases involved in the putative 3′ end interaction, reduced satC to undetectable levels. All three alterations tested in the two lowest positions on the LSL 3′ side still allowed substantial accumulation of satC in protoplasts similar to most of the partner positions on the 5′ side. Altogether, these results indicate that most positions within the middle and upper region of the LSL cannot be individually altered without substantially reducing satC accumulation in vivo. It is interesting to note that four carmoviruses (TCV, *Saguaro cactus virus*, *Japanese iris necrosis virus*, and *Hibiscus chlorotic virus*) have identical LSL sequences in their respective H5 hairpins while most other carmoviruses have related sequences that differ at symmetrical positions from that of TCV, mainly at the base of the LSL (Zhang et al., in press).

SatC containing single base changes in the LSL cause second site alterations in planta

To examine the effect of H5 LSL mutations on accumulation of satC in a natural host, individual mutants described in Fig. 2A were inoculated together with TCV onto each of three turnip seedlings. At 21 days post inoculation (dpi), satC present in total RNA preparations isolated from uninoculated leaves was amplified by RT-PCR and the resultant cDNAs cloned and sequenced. The results are summarized in Table 1 and Fig. 2A. With only one exception, all mutants that accumulated to less than 7% of wt levels in protoplasts either did not accumulate to PCR-detectable levels in plants or some or all clones recovered contained reversions to wt (Fig. 2A, subscripts N, R, and R/S; Table 1). The most damaging mutations, for which no progeny were detected, are located on the 3′ side of the LSL, in or near the region proposed to interact with the 3′ end to repress minus-strand synthesis (U296C; G298A). SatC containing A281G gave rise to progeny that maintained the alteration in plants despite having undetectable accumulation protoplasts. However, only trace amounts of the satRNA were visible in ethidium bromide-stained gels of total RNA preparations from infected plants (data not shown; satC accumulates to the level of 5S ribosomal RNA in infected plants and is easily detectable in ethidium bromide-stained gels).

Nine of ten mutations that permitted accumulation of satC to at least 7% of wt levels in protoplasts were either stably maintained in plants or showed only some reversion to wt (Fig. 2A; Table 1). SatC containing U285A, which accumulated to 8% of wt levels, reverted to either the wt base (8 of 12 clones) or to a cytidylate (4 of 12 clones). Similarly, five of six progeny clones isolated from plants inoculated with satC containing A281C had a uridylate at this position while one contained a reversion to the wt adenylate (note that A281U was a stable alteration in plants; Fig. 2A). Altogether, these results support a sequence-specific requirement for nearly all residues in the middle and upper portion of the LSL for robust satC accumulation in plants and protoplasts.

Sequencing of 25 full-length satC clones derived from six plants inoculated with wt satC revealed no mutations in 7750 bases analyzed. Of the 127 full-length satC clones derived from mutants with alterations in the H5 LSL, six different second-site changes were found in five clones isolated from four different plants. One progeny clone derived from satC containing U301A had a reversion of the original mutation and an adenylate to guanylate transition at position 215 in the

Table 1
Summary of progeny derived from satC containing mutations in the H5 LSL

Name	Maintained mutations	Reversions	Second site mutations[a]	Location of second site mutations[b]
U285A	0	12[c]	1(1)	U285-1: U285C, A282G
U285G	0	5	0	
U285C	2	0	0	
A284C	0	6	0	
A283G	0	3	0	
A283C	0	4	0	
A283U	0	9	0	
A282U	4	0	0	
A281G	2	0	0	
A281C	0	6[d]	0	
A281U	5	0	0	
U280A	1	3	0	
U280G	1	1	0	
U280C	0	2	0	
C279A	6	0	0	
C279G	4	1	0	
C279U	5	0	0	
U296C	0	0	0	
G297A	0	7	0	
G297C	0	5	2 (5)	G297C-1: C300G, G230A G297C-2: C300G, G230A, ΔCU between C264 and U269
G298A	0	0	0	
G298C	0	4	0	
G299A	0	4	0	
C300G	4	1	1 (2)	C300G-1: U302G, G230A
C300U	2	2	0	
U301A	2	2	1 (1)	U301A-1: A215G
U302A	5	0	0	
U302G	5	0	0	

[a] The number of clones that contained second site mutations with the number of second site mutations found in all progeny clones in parentheses.
[b] Name of the clone: bases altered.
[c] Eight clones reverted to wt, four clones had an adenylate to cytidylate transversion.
[d] One clone reverted to wt, five clones had a cytidylate to uridylate transition.

middle of five consecutive adenylates near the base of M1H (Table 1; Fig. 3A). An adenylate to guanylate transition was also found for a single progeny of satC containing U285A, which additionally contained a primary site alteration to a cytidylate. The second site mutation was at position 282 in the LSL (A282G). Because the function of the 5′ side of the LSL is unknown, it is not clear how or if this second site change compensated for the original mutation.

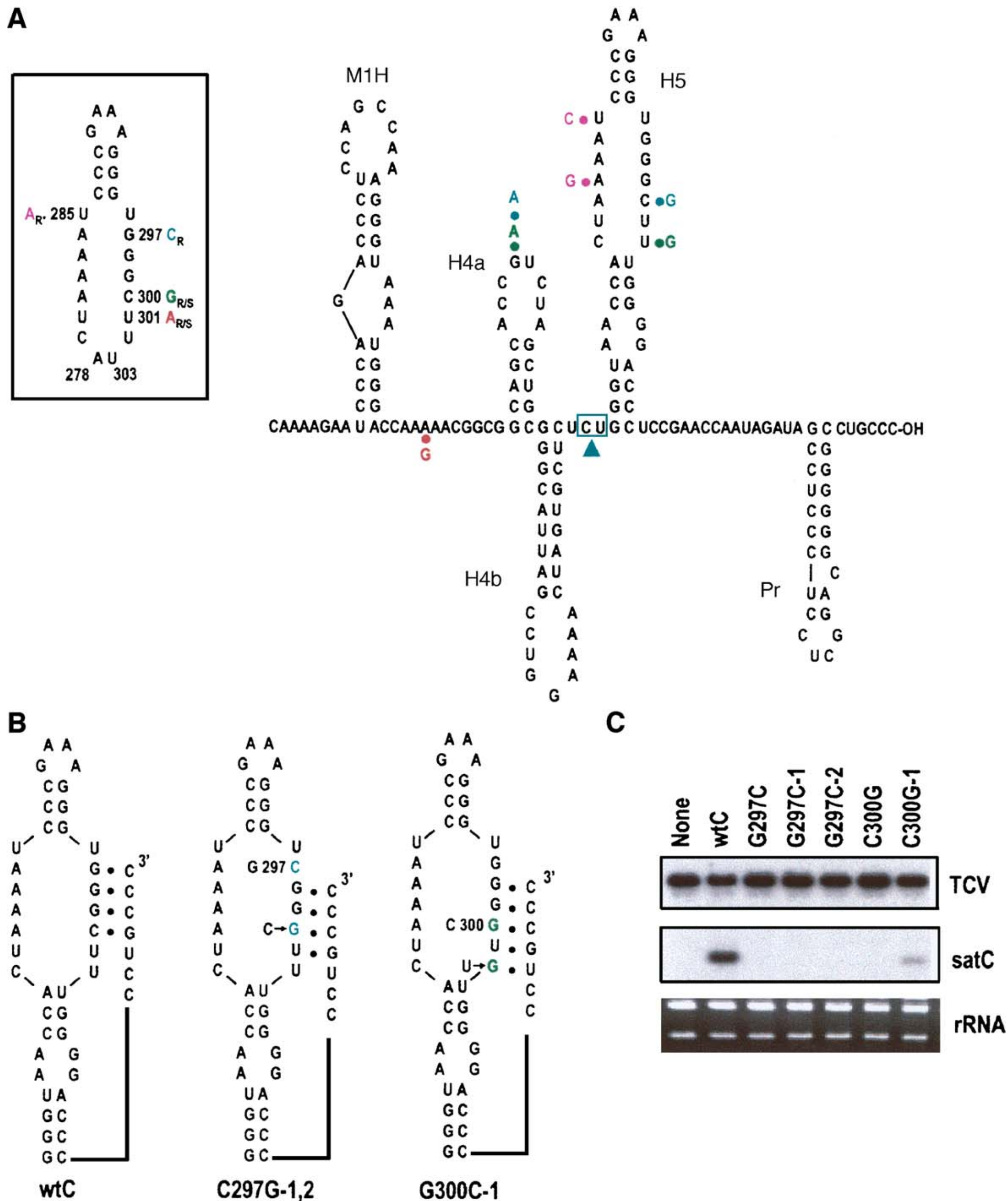

Fig. 3. Location of second site mutations in the progeny of satC H5 LSL mutants. (Inset) The primary mutations in H5 that gave rise to second site mutations. R, S, R/S, and R* subscripts were described in the legend to Fig. 2. Second site mutations and their primary site progenitors are color-coded. A two-base deletion found in progeny G297C-2 (Table 1) is marked with a triangle and boxed. Because this region contains three tandem CU bases, which bases were deleted cannot be determined. (B) Possible contribution of second site changes within H5 to strengthening base pairing of the LSL 3′ side and the 3′ terminus of satC. Progenitor mutations are indicated with their position number. Second site alterations are denoted by arrows preceded by the wt base. Names of the mutant clones containing the second site alterations are given below the structures. (C) Representative RNA gel blot of wt and mutant parental and progeny satC in protoplasts at 40 hpi. Ethidium bromide staining of the gel before blotting shows rRNA loading control (panel below the blot). None, no added satC. wtC, wt satC.

Two clones derived from the same plant infected with satC containing G297C had reversions of the original mutations and multiple similar second site alterations (Table 1): progeny clone G297C-1 had a cytidylate to guanylate transversion within the LSL at position 300 and a guanylate to adenylate transition at position 230 in the loop of another hairpin, H4a (Fig. 3A). Progeny clone G297C-2 contained these two alterations as well as a deletion of two bases between H4b and H5. The second site change within the LSL in these two related progeny clones could help to reestablish base pairing with the 3′ end before reversion of the original mutation (Fig. 3B, middle). SatC containing C300G also produced a progeny clone (C300G-1) with similar second site alterations; a uridylate to guanylate transversion within the LSL at position 302 and a second mutation identical to that previously described in the loop of H4a (G230A). The alteration within the LSL could also strengthen base pairing with the 3′ end that would be disrupted by the original mutation (Fig. 3B, right).

C300G-1 was the only clone derived from C300G that did not contain a reversion of the original mutation, suggesting that the second site changes were compensatory. To test this possibility, the parental satC containing C300G and progeny clone C300G-1 were assayed for accumulation in protoplasts. At 40 hpi, only C300G-1 accumulated to detectable levels (19% of wt satC) (Fig. 4D), supporting a compensatory effect for the second site alterations. The two clones derived from satC containing G297C were also tested for accumulation in protoplasts. However, neither the parental construct nor the progeny clones accumulated to detectable levels.

Examination of a possible interaction between the H5 LSL and the loop of H4a

The finding of identical guanylate to adenylate transitions within the loop of H4a in three clones derived from two different LSL mutants (C300G and G297C) suggested that this alteration might be compensating for the original mutations. While H4a has no known function, a structurally identical hairpin can exist at the same position relative to H5 and H4b in TCV and the related carmovirus *Cardamine chlorotic fleck virus* (CCFV) (Fig. 4A and data not shown). Analysis of the 3′ side of the satC, TCV and CCFV LSLs and their respective H4a terminal loop sequences revealed possible base pairing involving four (CCFV) or five positions (TCV and satC) that would be disrupted by the primary mutations in satC (Fig. 4A). While these LSL bases have been previously shown to interact with the satC 3′ end, it is possible that the loop of H4a might serve as a derepressor, to help release the LSL from the 3′ end by interacting with the LSL. The second site alteration in the H4a loop could help to reestablish base pairing disrupted by the primary C300G and G297C mutations (Fig. 4B).

To provide evidence for or against this possible interaction, mutations were introduced into the loop of satC H4a that either preserved (U231C, C232U, C300G/G230C), disrupted (U231A, C232A), or reduced (G230C) the putative base pairing shown in Fig. 4C. SatC with H4a alterations U231A or C232A accumulated to near wt levels in protoplasts, suggesting that disruption of this putative H4a/LSL interaction was not detrimental to satC accumulation (Fig. 4D). However, G230C and U231C reduced accumulation of satC by 33% and 31%, respectively, suggesting a role for H4a in satC accumulation in protoplasts. The compensatory exchange between the LSL and H4a (C300G/G230C) was highly detrimental to satC accumulation (Fig. 4D), indicating that addition of G230C did not compensate for the previously found reduction in satC levels due to C300G (Fig. 2A). Therefore, while these results suggest a role for H4a in satC accumulation, they do not at this time support the specific interaction presented in Fig. 4A between H4a loop residues and the H5 LSL.

In vivo genetic selection of the satC H5 LSL

Analysis of RNA structures by site-specific mutagenesis provides limited (and sometimes incorrect) information on the importance of specific residues because the alterations are tested in the context of remaining wt sequences (Carpenter and Simon, 1998). In other words, specific alterations deemed detrimental in the environment of wt sequences may not necessarily be detrimental if other bases in the structure (in addition to compensatory exchanges) are also altered. This may be especially true for internal symmetrical loops, where non-Watson–Crick base pairs likely permit continued interaction between the two strands due to stabilization by one or more hydrogen bonds between partners as well as same or cross-strand stacking. If the structure of an internal loop is required for hairpin function, these non-Watson–Crick base pairs might be replaceable by other canonical or noncanonical base pairs provided that they are isosteric with the original base pairs (Leontis et al., 2002b).

Therefore, to determine more precisely the necessity for specific bases in the LSL, the complete LSL sequence was subjected to in vivo genetic selection (in vivo SELEX). As described in Materials and methods, plants were inoculated with TCV and a pool of satC sequences containing completely randomized LSL sequence, which allowed for side-by-side functional selection as well as sequence evolution in multiple rounds of infections. For the first-round SELEX, the 14 bases of the LSL were randomized by PCR using degenerate oligonucleotides. SatC transcripts synthesized directly from the PCR products were inoculated onto 60 turnip seedlings along with TCV genomic RNA. At 21 dpi, viable satC species were recovered by RT-PCR from RNA extracted from uninoculated leaves and full-length satC was cloned and sequenced.

Only 2 of the 60 infected turnip plants displayed satC symptoms (stunting and highly crinkled, dark green leaves) and only those plants contained satC detectable by PCR. Seventeen clones derived from RNA accumulating in the

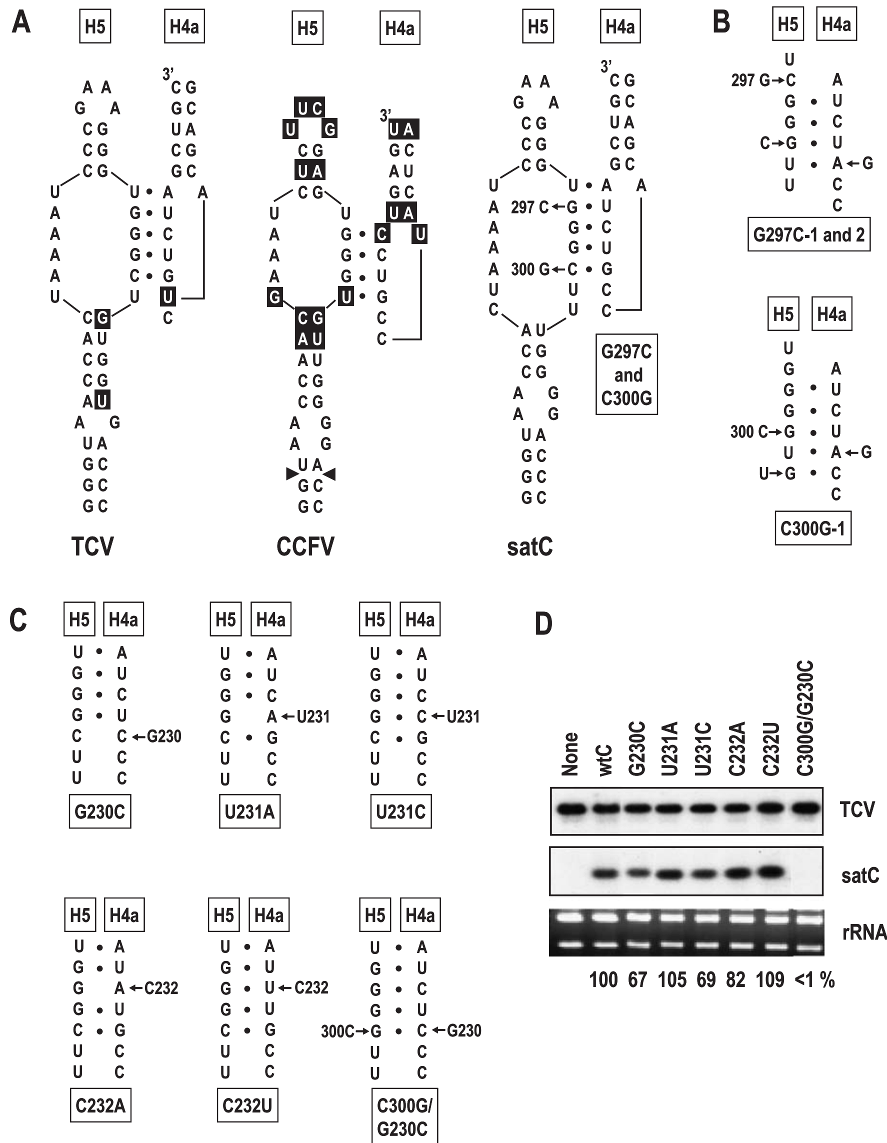

Fig. 4. Mutational analysis of a possible H5/H4a interaction in satC. (A) Possible base pairing between satC H5 LSL and the loop of H4a. The alterations generating parental constructs G297C and C300G, which should disrupt this base pairing, are shown. Differences between satC H5 and H5 of TCV and CCFV are boxed. (B) Predicted base pairing between H5 LSL and the loop of H4a in progeny of G297C (G297C-1 and G297C-2) and C300G (C300G-1) which contain second site alterations. Wt satC bases with positional numbers are shown with arrows pointing to the parental G297C (top) and C300G (bottom) alterations. Second site changes are similarly designated but without positional numbers. Progeny clones G297C-1 and G297C-2, derived from G297C in the same plant, differed from each other by G297C-2 having an additional two-base deletion upstream of H5 (see Fig. 3). Potential reestablishment of base pairing due to the second site alterations in G297C-1, -2, and C300G-1 are shown. (C) Series of satC constructs containing mutations designed to disrupt or maintain base pairing between H5 and H4a. (D) Representative RNA gel blot of wt and mutant satC accumulation in protoplasts at 40 hpi. Ethidium bromide staining of the gel before blotting shows rRNA loading control (panel below the blot). Values below the panels are percentages of wt levels of accumulation (average of three independent experiments). None, no added satC. wtC, wt satC.

two plants contained five different LSL sequences (Table 2, Fig. 5A). These first-round winners displayed strong sequence conservation with the wt LSL sequence, especially in the middle and upper portions of the loop. Eight positions (A281, A283, A284, and 296UGGGC300) were identical to wt bases in all clones and A282 was present in 12 of 17 clones. This included the GGGC on the 3′ side of the LSL that interacts with the 3′ end in vitro (Zhang et al., in press). Either the wt uridylate or a cytidylate was acceptable at position 285. A cytidylate in this position was previously found to be stably maintained in plants and only reduced accumulation of satC by 40% in protoplasts (Fig. 2A). All clones contained two or three differences from wt at the base of the LSL, the region previously found to be more tolerant to alterations (Fig. 2A). The guanylate found at position 302 in two clones is also present in the H5 LSL of TCV and was found to enhance satC accumulation in protoplasts by 28% (Fig. 2A).

Table 2
Summary of in vivo SELEX for the LSL

	Clone[a]	LSL[b]		Plant[c]						Total
		5′ side	3′ side	1	2	3	4	5	6	
Round 1	1	*G*UA*G*AAU	UGGGC*GG*	5						5
	2	*G*UAAAAU	UGGGC*GG*	4						4
	3	*A*UAAAA*C*	UGGGC*G*U		3					3
	4	*AG*AAAA*C*	UGGGC*G*U		3					3
	5	*AG*AAAAU	UGGGC*G*U		2					2
	Total clones assayed from each plant			9	8					17
Round 2	3	*A*UAAAA*C*	UGGGC*G*U	2	7	7	6	9	4	35
	6	*A*UAAAAU	UGGGC*G*U		1	1			3	5
	7	*G*UAAAAU	UGGGC*G*U					2		2
	Total clones assayed from each plant			2	8	8	6	11	7	42
Round 3	6	*A*UAAAAU	UGGGC*G*U	1	2	4	4	4	3	18
	8	*A*UAAAAC	UGGGCUU	1	2		2	3	2	10
	3	*A*UAAAA*C*	UGGGCGU	1	2		1			4
	Total clones assayed from each plant			3	6	4	7	7	5	32

[a] From Fig. 5A.
[b] Sequence is presented 5′ to 3′. Bases that differ from wt satC LSL are underlined in italic.
[c] The number of clones found in each plant at 21 dpi.

For the second round, equal amounts of total RNA isolated from all 60 plants of the previous round were pooled and re-inoculated onto six turnip seedlings, and progeny recovered and sequenced at 21 dpi. Thirty-five of 42 clones recovered were identical to one first-round winner (clone 3) (Fig. 5A). Two additional sequences (clones 6 and 7) had not previously been isolated. All winners contained either G:U, U:G, or A:U pairs at the base of the LSL, indicating that canonical base pairs, while not present in wt satC, are acceptable in this location, supporting the conclusions of the site-specific mutagenesis analysis.

Equal amounts of total RNA isolated from second-round plants were combined and used to inoculate six more plants. For this third, and final SELEX round, three sequences were recovered, including the best winner from the second round (clone 3). Clone 6, which was a less prevalent second-round winner, emerged as the most recovered third-round winner. A new sequence was also recovered in the third round (clone 8) that likely evolved from clone 3 by a single change from a guanylate to the wt uridylate at position 302.

Because the number of satC with a particular sequence recovered in later rounds of in vivo SELEX can be influenced by the starting concentration of each sequence in plants of the previous round, the third-round winners were subjected to side-by-side competition for fitness starting with equal amounts of individual transcripts. Also included in this competition was a randomly selected first-round winner (clone 1). At 21 dpi, satC species were cloned and sequenced from three infected plants. Twenty-nine of thirty-one clones were identical to clone 6, and the remaining two clones were clone 8 (Table 3). The fitness order of the third-round winners was therefore clone 6, clone 8, and then clone 3.

Clone 6 differed from wt satC at two positions (C279A and U301G). While the U301G alteration was not tested in the site-specific mutagenesis analysis, satC containing the C279A alteration accumulated 34% better than wt satC in protoplasts (Fig. 2A). To determine the fitness of clone 6 compared with wt satC in plants, equal amounts of wt and mutant transcripts were combined and inoculated onto three plants along with TCV. Twenty-three of the twenty-six recovered clones were wt satC (Table 3) indicating that one or both of the base differences in clone 6 reduced fitness of satC in plants.

Fitness of satC variants to accumulate in plants depends on several factors including replication competence, stability, and ability to enhance the movement of TCV (Sun and Simon, 2003; Zhang and Simon, 2003a, 2003b). To determine if the fitness of the in vivo SELEX winners to accumulate in plants correlated with their ability to accumulate in protoplasts, the three third-round winners, together with first-round clone 1 and satC containing a randomly selected sequence from the original randomized population (Rd), were separately inoculated onto protoplasts along with TCV. By assaying accumulation in protoplasts, this allowed for a determination of replication/stability in the absence of movement. All three third-round winners accumulated to near wt levels in protoplasts (Figs. 5B and C), while the first-round winner (clone 1) and the randomly selected satC (Rd) did not accumulate to detectable levels. Because we have never identified mutations in satC that affect the stability of the satRNA, these results suggest that the ability of the SELEX winners to replicate was a primary factor for fitness in plants. However, while all third-round winners accumulated to near wt levels in protoplasts, clones 3 and 8 were substantially less fit than clone 6 in the competition assay. Furthermore, wt satC was considerably more fit in plants than clone 6 yet replication levels in protoplasts were very similar. This suggests that fitness of in vivo SELEX winners with different LSL sequences in plants depends on factors in addition to those that allow robust replication in protoplasts.

Discussion

Negative regulation of minus-strand synthesis by a repressor has been identified for TCV (Zhang et al., in press), *Tomato bushy stunt virus* (TBSV) (Pogany et al., 2003) and predicted for *Barley yellow dwarf virus* (Koev et al., 2002). In TCV and satC, the four 3′ end terminal bases can form Watson–Crick base pairs with the 3′ side of the H5 LSL, thus presumably sequestering the 3′ end from the RdRp. A second sequence, located in a single-stranded region upstream of H5, was predicted to function as a derepressor by disrupting the 3′ end–H5 interaction (Zhang et al., in press).

To explore the sequence requirements of the LSL, we performed both single site mutational analysis and in vivo SELEX. The results of these two approaches were very

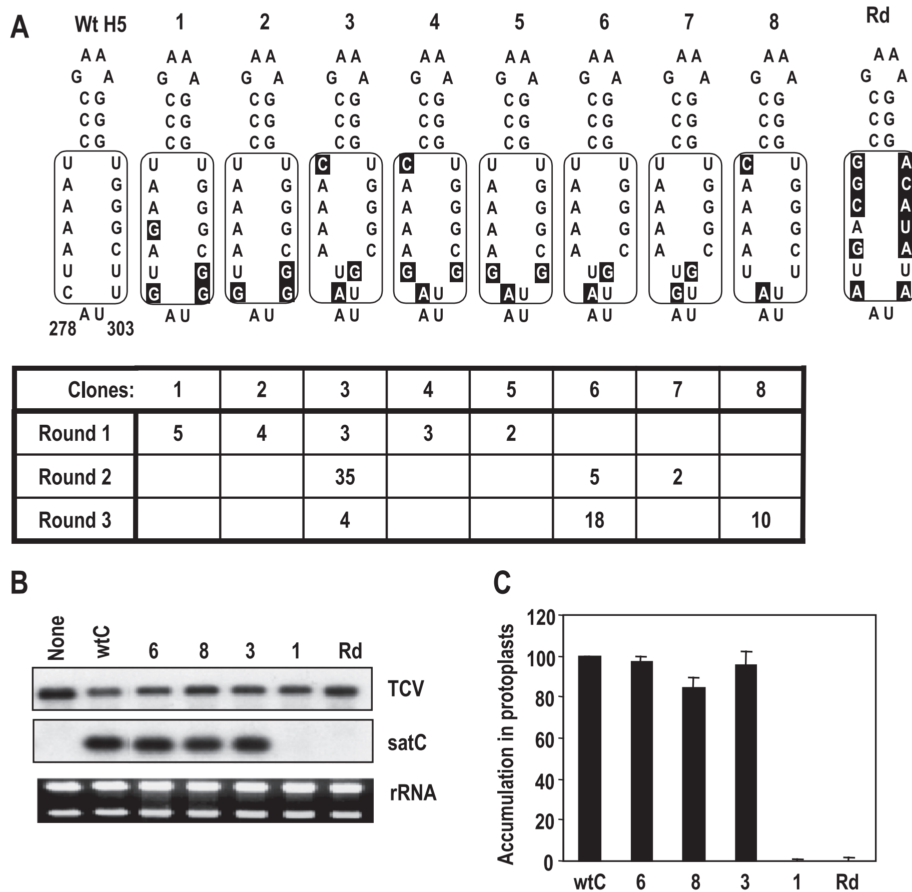

Clones:	1	2	3	4	5	6	7	8
Round 1	5	4	3	3	2			
Round 2			35			5	2	
Round 3			4			18		10

Fig. 5. In vivo SELEX of the satC H5 LSL. (A) Sequences recovered from three rounds of selection. Sequence names (numbers) are indicated above each structure. Bases that differ from wt satC in progeny clones 1–8 are boxed. Number of clones containing each sequence recovered per round is indicated in the table. (B) Representative RNA gel blot of total RNA extracted from *Arabidopsis* protoplasts at 40 h after inoculation with TCV and wt satC or various SELEX winners. All third-round sequences were selected for analysis along with one first-round winner (sequence 1) and satC containing a randomly selected H5 LSL sequence (Rd). wtC, wt satC. Ethidium bromide staining of the gel before blotting shows ribosomal RNA loading control (panel below the blot). (C) Averaged values for accumulation of satC SELEX winners in protoplasts. Values represent results from three independent experiments. Standard deviations are indicated.

consistent. On the 5′ side of the LSL, there was strong conservation of the four consecutive adenylates and for a pyrimidine at position 285. The residues opposite these positions on the 3′ side of the LSL were conserved in all recovered SELEX clones and alterations were either poorly or not conserved in satC accumulating in plants. The importance of these 3′ side residues supports our model that the 3′ terminal satC sequence (GCCC-OH) base pairs with sequence in the 3′ side of the LSL. The lower positions of the LSL were considerably more flexible, with both canonical (A:U, G:U, and C:G) and noncanonical (G•G) pairings able to replace the wt C•U in the lowest position and U:G and G•G pairs able to replace the U•U pairing in the penultimate position. Interestingly, TCV contains a C:G at the base of its LSL while the related carmovirus CCFV has several additional canonical base pairings in the same region of its LSL.

Table 3
Competition between third-round SELEX winners and wt satC

	Clone[a]	Plant[b]			Total
		1	2	3	
Competition 1	6	7	8	14	29
	8	1		1	2
	3				
	1				
Competition 2	wt satC	6	5	12	23
	6	1	2		3

[a] From Fig. 5A.
[b] The number of clones found in each plant at 21 dpi.

Because wt satC was more fit than our best SELEX winner (clone 6), a question that arises is why clones containing wt satC sequence were not recovered from the in vivo SELEX. The initial randomized population of cDNA (4×10^{12} cDNA fragments used for in vitro transcription per plant) was more than sufficient to contain all possible sequences in the 14 positions. However, the actual number of RNAs that enter cells and initiate infection is not known. This would suggest that the majority of satRNA sequences inoculated onto plants would not be part of the initial selection, reducing the pool of possible sequence combinations below that re-

quired to assay every sequence. In a previous in vivo SELEX of a 14-base satC motif that was determined to have only 12 specific bases, wild-type sequence was recovered in the first round (Guan et al., 2000b). In vivo SELEX thus provides information on what sequences can support accumulation but not always on the identity of the best possible sequence.

Results from in vivo SELEX suggest that H5 has a role in satC fitness in addition to permitting robust replication. All third-round winners replicated to near wt levels, while fitness in plants varied substantially. A recently completed in vivo SELEX of the M1H, a replication enhancer in its minus-sense orientation, also indicated that sequences were recovered with a role in addition to replication (Zhang and Simon, 2003a, 2003b). While replication-related motifs were recovered in minus-sense RNA, a sequence nonspecific hairpin in plus strands strongly influenced satC fitness by bringing together flanking sequences that interfered with virion formation, which enhanced the ability of TCV to suppress RNA silencing. What additional satRNA property might be influenced by H5 is not known. In a recent investigation of the H5 LSL of TCV, mutations in many positions were also not stable. Surprisingly, 25% of mutant TCV progeny had one to three second site alterations scattered throughout 200–300 bases in the 3′ UTR in addition to a reversion of the original alterations. Interestingly, the second site changes were strongly biased towards uridylate to cytidylate and adenylate to guanylate transitions (McCormack and Simon, in press). These results led to the speculation that the TCV H5 also functions as an RNA chaperone required for proper assembly of the RdRp.

The second site changes found in progeny of some satC LSL mutants did not display the same bias or random positioning as the TCV mutants, and some could be hypothetically connected to compensating for the original alterations. The benefit of the G230A second site change found in the loop of H4a in progeny of two LSL mutants, however, is not understood. While our results do not support one possible interaction between H4a and H5 (Fig. 4), it remains possible that a less obvious relationship exists between H4a and either H5 or sequences that interact with H5.

The minus-strand repressor in TBSV (SL3) contains an internal loop with both similarities and striking differences with the carmoviral H5. Whereas all carmoviral H5 large internal loops are symmetrical or nearly symmetrical, the TBSV SL3 is asymmetrical, with only a single adenylate occupying the 5′ side (Pogany et al., 2003). The 3′ side of the SL3 and H5 internal loops are similar, with five of eight SL3 bases (GGGCU) identical to their carmoviral counterparts. The requirement for symmetry (or near symmetry) in the H5 internal loop of carmoviruses is not known. The LSL is uncommonly large for an interior symmetrical loop. Other examples of large symmetrical internal loops include loop E of 5S rRNA (14 bases, Specht et al., 1991), the sarcin/ricin loop of 23S rRNA (10 bases; Leontis et al., 2002a), internal loops within ADAR substrates (12 bases, Lehmann and Bass, 1999), and the internal loop in group I introns (10 bases, Cech et al., 1994). Biochemical analyses of the similarly sized loop E suggest that the loop adopts a lightly overwound but still roughly helical structure that is required for ribosomal protein L25 binding (Tang and Draper, 1994). Internal loops play important structural and functional roles in RNA, providing flexibility and allowing RNAs to form more compact structures (Jaeger et al., 1993; Zacharias and Hagerman, 1996). Why carmoviruses appear to require symmetry in the internal loops of their repressors while tombusviruses do not will only be answered when detailed three-dimensional structures are available for both hairpins.

Materials and methods

Construction of satC mutants

Mutations were introduced into the satC H5 LSL by PCR using a plasmid containing wt satC cDNA downstream from a T7 RNA polymerase promoter (pT7C+) (Song and Simon, 1994). For mutations in the 5′ side of the LSL, primers were homologous to positions 257–300 and complementary to positions 337–356 (oligo 7). The former primer contained a ratio of 76% wt bases and 8% of each of the other bases at positions 279–285. For construction of additional mutations in position 279 to 281, primers were oligo 7 and homologous to positions 257–294. The latter primer contained an equal mixture of bases at positions 279–281. Following digestion with *Spe*I and *Sma*I, the fragment was inserted into the analogous location in pT7C+, which had been treated with the same restriction enzymes. For mutations in the 3′ side of the LSL, primers contained a T7 RNA polymerase promoter and positions 1–14 of satC (T7C5′) or were complementary to positions 276–356. The latter primer contained 76% wt base and 8% of each of the other bases at positions 296–302. For additional mutations at positions 296 and 302, primers used were T7C5′ and complementary to positions 276–356 with positions 296 and 302 containing an equal mixture of bases. PCR products were ligated into the *Sma*I site of pUC19.

Mutations were introduced into the terminal loop of satC H4a by PCR using pT7C+ and primers homologous to positions 1–14 and complementary to positions 220–263. The latter oligonucleotide contained G at position 230, T or G at position 231, or T or A at position 232. PCR products were subsequently digested with *Spe*I and *Sna*BI and cloned into pT7C+ replacing the analogous wt fragment. To generate satC containing mutations in both H5 and H4a, construct G230C was digested with *Spe*I and *Sna*BI, and the small fragment cloned into construct C300G that had been treated with the same restriction enzymes.

pNco-C277, which was used for in vivo SELEX, was generated by PCR using pNco-C (Simon et al., 1988) and primers C5′ and oligo 277, complementary to positions 261–277. PCR products were cloned into the *Sma*I site of pUC19.

In vitro transcription, plant inoculations, and cloning and sequencing of progeny virus

TCV genomic RNA and satC were synthesized using T7 RNA polymerase and plasmids linearized with *Sma*I, which generates transcripts with precise 5′ and 3′ ends. Three 2-week-old turnip seedlings were inoculated with satC mutant transcripts (0.4 μg/plant) along with TCV genomic RNA (4 μg/plant). Total RNA was extracted from uninoculated leaves at 21 dpi. SatC-sized species were amplified by RT-PCR using primers C5′ and oligo 7 and cloned into the *Sma*I site of pUC19. Complete full-length sequences were determined for each clone (excluding the primer sequences used for cloning).

In vivo SELEX

In vivo SELEX was performed as previously described (Carpenter and Simon, 1998; Guan et al., 2000a, 2000b; Sun and Simon, 2003; Zhang and Simon, 2003a, 2003b). Full-length satC cDNAs containing randomized bases in the H5 LSL were generated by PCR using pNco-C277 as template. Primers used were T7C5′ and 3CLS, which is complementary to positions 261–356. Within this primer, positions 279–285 and 296–302 contained randomized sequence. PCR products were purified and directly subjected to in vitro transcription using T7 RNA polymerase. The number of cDNA molecules used for in vitro transcription of RNA to infect one plant was 4×10^{12}.

For the first SELEX round, 5 μg of satC transcripts containing randomized LSL sequence were inoculated onto each of 60 turnip seedlings along with 4 μg of TCV transcripts. Total RNA was extracted from uninoculated leaves at 21 dpi. Viable satC species were recovered by RT-PCR using primers C5′ and oligo 7, cloned into the *Sma*I site of pUC19 and sequenced. For the second round, equal amounts of leaf tissue from the 60 plants was combined, total RNA extracted, and then inoculated (approximately 5 μg/plant) onto six turnip seedlings. For the third round, equal amounts of total RNA, extracted from each plant of the previous round, was pooled and then inoculated onto six turnip seedlings (approximately 5 μg/plant). SatC species at 21 dpi were cloned and full-length sequences determined.

Protoplast preparation, inoculation, and RNA gel blots

SatC transcripts were synthesized from plasmids linearized with *Sma*I (for mutations in H5 and H4a) or directly from PCR products (for SELEX winners, using primers T7C5′ and oligo 7) using T7 RNA polymerase. Protoplasts (5×10^6), prepared from callus cultures of *A. thaliana* ecotype Col-0, were inoculated with 20 μg of TCV genomic RNA transcripts with or without 2 μg of satC RNA transcripts using PEG-$CaCl_2$, as previously described (Kong et al., 1997). Total RNA isolated from protoplasts at 40 hpi was subjected to RNA gel blot analysis. The RNA was probed with a [γ-^{32}P]-ATP-labeled oligonucleotide complementary to both positions 3950–3970 of TCV genomic RNA and positions 259–269 of satC (Zhang and Simon, 2003a, 2003b).

Competition of SELEX winners in plants

For competition between wt satC and sequence 6, equal amounts of transcripts of wt satC and sequence 6 were combined and used to inoculate three turnip seedlings (0.4 μg/plant) along with TCV genomic RNA transcripts (4 μg/plant). For competition among the four SELEX winners, equal amounts of transcripts of each competitor were combined and used to inoculate three turnip seedlings (0.4 μg/plant) along with TCV genomic RNA transcripts (4 μg/plant). SatC species from all plants at 21 dpi were cloned and assayed as described above.

Acknowledgments

Funding was provided by grants from the U.S. Public Health Service (GM61515-01) and the National Science Foundation (MCB-0086952) to AES.

References

Barton, D.J., O'Donnell, B.J., Flanegan, J.B., 2001. 5′ Cloveleaf in poliovirus RNA is a *cis*-acting replication element required for negative-strand synthesis. EMBO J. 20, 1439–1448.

Buck, K.W., 1996. Comparison of the replication of positive-stranded RNA viruses of plants and animals. Adv. Virus Res. 47, 159–251.

Carpenter, C.D., Simon, A.E., 1998. Analysis of sequences and putative structures required for viral satellite RNA accumulation by in vivo genetic selection. Nucleic Acids Res. 26, 2426–2432.

Carrington, J.C., Heaton, L.A., Zuidema, D., Hillman, B.I., Morris, T.J., 1989. The genome structure of Turnip crinkle virus. Virology 170, 219–226.

Cech, T.R., Damberger, S.H., Gutell, R.R., 1994. Representation of the secondary and tertiary structure of group I introns. Nat. Struct. Biol. 1, 273–280.

Chapman, R.M., Kao, C.C., 1999. A minimal RNA promoter for minus-strand RNA synthesis by the brome mosaic virus polymerase complex. J. Mol. Biol. 286, 709–720.

Deiman, B.A.L.M., Koenen, A.K., Verlaan, P.W.G., Pleij, C.W.A., 1998. Minimal template requirements for initiation of minus-strand synthesis in vitro by the RNA-dependent RNA polymerase of turnip yellow mosaic virus. J. Virol. 72, 3965–3972.

Dreher, T.W., 1999. Functions of the 3′-untranslated regions of positive strand RNA viral genomes. Annu. Rev. Phytopathol. 37, 151–174.

Duggal, R., Lahser, F.C., Hall, T.C., 1994. Cis-acting sequences in the replication of plant viruses with plus-sense RNA genomes. Annu. Rev. Phytopathol. 32, 287–309.

Fabian, M.R., Na, H., Ray, D., White, K.A., 2003. 3′-Terminal RNA secondary structures are important for accumulation of Tomato bushy virus DI RNAs. Virology 313, 567–580.
Guan, H., Carpenter, C.D., Simon, A.E., 2000a. Analysis of *cis*-acting sequences involved in plus-strand synthesis of a TCV-associated satellite RNA identifies a new carmovirus replication element. Virology 268, 345–354.
Guan, H., Carpenter, C.D., Simon, A.E., 2000b. Requirement of a 5′-proximal linear sequence on minus-strand for plus-strand synthesis of a satellite RNA associated with TCV. Virology 268, 355–363.
Hacker, D.L., Petty, I.T.D., Wei, N., Morris, T.J., 1992. Turnip crinkle virus genes required for RNA replication and virus movement. Virology 186, 1–8.
Haldeman-Cahill, R., Daros, J.A., Carrington, J.C., 1998. Secondary structures in the capsid protein coding sequence and 3′ nontranslated region involved in amplification of the tobacco etch virus genome. J. Virol. 72, 4072–4079.
Herold, J., Andino, R., 2001. Poliovirus RNA replication requires genome circularization through a protein–protein bridge. Mol. Cell 7, 581–591.
Jaeger, J.A., Santalucia, J., Tinoco, I., 1993. Determination of RNA structure and thermodynamics. Annu. Rev. Biochem. 62, 255–287.
Khromykh, A.A., Meka, H., Guyatt, K.J., Westaway, E.G., 2001. Essential role of cyclization sequences in flavivirus RNA replication. J. Virol. 75, 6719–6728.
Klovins, J., Berzins, V., van Duin, J., 1998. A long-range interaction in Q-beta RNA that bridges the thousand nucleotides between the M-site and the 3′ end is required for replication. RNA 4, 948–957.
Koev, G., Liu, S., Beckett, R., Miller, W.A., 2002. The 3′-terminal structure required for replication of Barley yellow dwarf virus RNA contains an embedded 3′ end. Virology 292, 114–126.
Kong, Q., Wang, J., Simon, A.E., 1997. Satellite RNA-mediated resistance to Turnip crinkle virus in *Arabidopsis* involves a reduction in virus movement. Plant Cell 9, 2051–2063.
Lehmann, K.A., Bass, B.L., 1999. The importance of internal loops within RNA substrates of ADAR1. J. Mol. Biol. 291, 1–13.
Leontis, N.B., Stombaugh, J., Westhof, E., 2002a. Motif prediction in ribosomal RNAs. Lessons and prospects for automated motif prediction in homologous RNA molecules. Biochimie 84, 961–973.
Leontis, N.B., Stombaugh, J., Westhof, E., 2002b. The non-Watson–Crick base pairs and their associated isostericity matrices. Nucleic Acids Res. 30, 3497–3531.
Li, W.-Z., Qu, F., Morris, T.J., 1998. Cell-to-cell movement of turnip crinkle virus is controlled by two small open reading frames that function in trans. Virology 244, 405–416.
McCormack, J., Simon, A.E., 2004. Biased hypermutagenesis of an RNA virus associated with mutations in an untranslated hairpin. J. Virol. (in press).
Melchers, W.J.G., Henderop, J.G.J., Slot, H.J.B., Pleij, C.W.A., Pilipenko, E.V., Agol, V.L., Galama, J.M.D., 1997. Kissing of two predominant hairpin loops in the coxsackie B virus 3′ untranslated region is the essential structural feature of the origin of replication required for negative-strand RNA synthesis. J. Virol. 71, 686–696.
Nagy, P.D., Pogany, J., Simon, A.E., 1999. RNA elements required for RNA recombination function as replication enhancers in vitro and in vivo in a plus-strand RNA virus. EMBO J. 18, 5653–5665.
Nagy, P.D., Pogany, J., Simon, A.E., 2001. In vivo and in vitro characterization of an RNA replication enhancer in a satellite RNA associated with turnip crinkle virus. Virology 288, 315–324.
Panavas, T., Nagy, P.D., 2003. The RNA replication enhancer element of tombusvirus contains two interchangeable hairpins that are functional during plus-strand synthesis. J. Virol. 77, 258–269.
Pillai-Nair, N., Kim, K.H., Hemenway, C., 2003. Cis-acting regulatory elements in the Potato virus X 3′ non-translated region differentially affect minus-strand and plus-strand RNA accumulation. J. Mol. Biol. 326, 701–720.
Pogany, J., Fabian, M.R., White, K.A., Nagy, P.D., 2003. Functions of novel replication enhancer and silencer elements in tombusvirus replication. EMBO J. 22, 5602–5611.
Quadt, R., Ishikawa, M., Janda, M., Ahlquist, P., 1995. Formation of Brome mosaic virus RNA-dependent RNA polymerase in yeast requires coexpression of viral proteins and viral RNA. Proc. Natl. Acad. Sci. U.S.A. 92, 4892–4896.
Rajendran, K.S., Pogany, J., Nagy, P.D., 2002. Comparison of Turnip crinkle virus RNA-dependent polymerase preparations expressed in *Escherichia coli* or derived from infected plants. J. Virol. 76, 1707–1717.
Ray, D., White, K.A., 1999. Enhancer-like properties of an RNA element that modulates Tombusvirus RNA accumulation. Virology 256, 162–171.
Ray, D., White, K.A., 2003. An internally located RNA hairpin enhances replication of Tomato bushy stunt virus RNAs. J. Virol. 77, 245–257.
Simon, A.E., Howell, S.H., 1986. The virulent satellite RNA of Turnip crinkle virus has a major domain homologous to the 3′ end of the helper virus genome. EMBO J. 5, 3423–3428.
Simon, A.E., Engel, H., Johnson, R.P., Howell, S.H., 1988. Identification of regions affecting virulence, RNA processing and infectivity in the virulent satellite of Turnip crinkle virus. EMBO J. 7, 2645–2651.
Singh, R.N., Dreher, T.W., 1998. Specific site selection in RNA resulting from a combination of nonspecific secondary structure and -CCR-boxes: initiation of minus strand synthesis by turnip yellow mosaic virus RNA-dependent RNA polymerase. RNA 4, 1083–1095.
Sivakumaran, K., Kim, C., Tayon Jr., R., Kao, C.C., 1999. RNA sequence and secondary structural determinants in a minimal viral promoter that directs replicase recognition and initiation of genomic plus-strand RNA synthesis. J. Mol. Biol. 294, 667–682.
Song, C., Simon, A.E., 1994. RNA-dependent RNA polymerase from plants infected with turnip crinkle virus can transcribe (+)- and (−)-strands of virus-associated RNAs. Proc. Natl. Acad. Sci. U.S.A. 91, 8792–8796.
Song, C., Simon, A.E., 1995. Requirement of a 3′-terminal stem-loop in in vitro transcription by an RNA dependent RNA polymerase. J. Mol. Biol. 254, 6–14.
Specht, T., Wolters, J., Erdmann, V.A., 1991. Compilation of 5S rRNA and 5S rRNA gene sequences. Nucleic Acids Res. 19, 2189–2191 (Suppl.).
Stupina, V., Simon, A.E., 1997. Analysis in vivo of turnip crinkle virus satellite RNA c variants with mutations in the 3′-terminal minus-strand promoter. Virology 238, 470–477.
Sun, X., Simon, A.E., 2003. Fitness of a Turnip crinkle virus satellite RNA correlates with a sequence-nonspecific hairpin and flanking sequences that enhance replication and repress the accumulation of virions. J. Virol. 77, 7880–7889.
Tang, R.S., Draper, D.E., 1994. Bend and helical twist associated with a symmetric internal loop from 5S ribosomal RNA. Biochem. 33, 10089–10093.
Vlot, A.C., Neeleman, L., Linthorst, H.J.M., Bol, J.F., 2001. Role of the 3′-untranslated regions of Alfalfa mosaic virus RNA in the formation of a transiently expressed replicase in plants and in the assembly of virions. J. Virol. 75, 6440–6449.
White, K.A., Bancroft, J.B., Mackie, G.A., 1992. Mutagenesis of a hexanucleotide sequence conserved in potexvirus RNAs. Virology 189, 817–820.
Williams, G.D., Chang, R.Y., Brian, D.A., 1999. A phylogenetically conserved hairpin-type 3′ untranslated region pseudoknot functions in coronavirus RNA replication. J. Virol. 73, 8349–8355.
You, S., Falgout, B., Markoff, L., Padmanabhan, R., 2001. In vitro RNA synthesis from exogenous Dengue viral RNA templates requires long-range interactions between 5′- and 3′-terminal regions that influence RNA structure. J. Biol. Chem. 276, 15581–15591.
Yu, H., Grassmann, C.W., Behrens, S.-E., 1999. Sequence and structural elements at the 3′ terminus of bovine viral diarrhea virus genomic RNA: functional role during RNA replication. J. Virol. 73, 3638–3648.
Zacharias, M., Hagerman, P.J., 1996. The influence of symmetric internal loops on the flexibility of RNA. J. Mol. Biol. 257, 276–289.

Zhang, F., Simon, A.E., 2003a. Enhanced viral pathogenesis associated with a virulent mutant virus or a virulent satellite RNA correlates with reduced virion accumulation and abundance of free coat protein. Virology 312, 8–13.
Zhang, G., Simon, A.E., 2003b. A multifunctional Turnip crinkle virus replication enhancer revealed by in vivo functional SELEX. J. Mol. Biol. 326, 35–48.
Zhang, G., Zhang, J., Simon, A.E., 2004. Repression and derepression of minus-strand synthesis in a plus-strand RNA virus replicon. J. Virol. (in press).